The Astronomical Journal, 136:881–889, 2008 August doi:10.1088/0004-6256/136/2/881

OBSERVATIONS OF 1999 YC AND THE BREAKUP OF THE GEMINID STREAM PARENT

Toshihiro Kasuga[1,2] and David Jewitt[1]
[1] Institute for Astronomy, University of Hawaii, 2680 Woodlawn Drive, Honolulu, HI 96822, USA; kasugats@ifa.hawaii.edu, jewitt@ifa.hawaii.edu
[2] JSPS Research Fellow, National Astronomical Observatory of the Japan, National Institutes of Natural Sciences, 2-21-1 Osawa, Mitaka, Tokyo 181-8588, Japan
Received 2008 April 17; accepted 2008 May 16; published 2008 July 14

ABSTRACT

The Apollo asteroid 1999 YC may share a dynamical association with the Phaethon–Geminid Stream Complex (PGC) (Ohtsuka et al. 2008). Here, we present photometric observations taken to determine the physical properties of 1999 YC. The object shows a nearly neutral reflection spectrum, similar to but slightly redder than the related objects 3200 Phaethon and 2005 UD. Assuming an albedo equal to that of 3200 Phaethon, we find that the diameter is 1.4 ± 0.1 km. Time-resolved broadband photometry yields a double-peaked rotational period of 4.4950 ± 0.0010 h, while the range of the light curve indicates an elongated shape having a projected axis ratio of ∼1.9. Surface brightness models provide no evidence of lasting mass loss of the kind seen in active short-period cometary nuclei. An upper limit to the mass loss is set at $\sim 10^{-3}$ kg s^{-1}, corresponding to an upper limit on the fraction of the surface that could be sublimating water ice of $<10^{-3}$. If sustained over the 1000 yr age of the Geminid stream, the total mass loss from 1999 YC (3×10^7 kg) would be small compared to the reported stream mass ($\sim 10^{12}$–10^{13} kg), suggesting that the stream is the product of catastrophic, rather than steady-state, breakup of the parent object.

Key words: comets: general – minor planets, asteroids – meteors, meteoroids

1. INTRODUCTION

Breakup or disintegration is an apparently common end state for the nuclei of comets (Chen & Jewitt 1994; Boehnhardt 2004; Jewitt 2004). Meteoroid streams appear to result from this process, including some which are associated with parent bodies whose physical properties are those of asteroids, not obviously comets (Babadzhanov 1994; Jenniskens 2006). A leading example of the latter is the Apollo-type near-Earth asteroid 3200 Phaethon (1983 TB) which is dynamically associated with the Geminid meteoroid stream (Whipple 1983). Phaethon may be a dead or dormant comet, but its unusual blue reflection spectrum distinguishes it from most other well-studied cometary nuclei, and no outgassing or mass-loss activity has ever been reported (Hsieh & Jewitt 2005; Wiegert et al. 2008). Recently, Ohtsuka et al. (2006) suggested the existence of a "Phaethon–Geminid stream Complex (PGC)" which implies a big group of split cometary nuclei/fragments based on their dynamical similarity. They identified asteroid 2005 UD, classified as an Apollo type, as having a common origin with 3200 Phaethon (Ohtsuka et al. 2006). Subsequent photometry of 2005 UD revealed that it has unusual blue optical colors like those of Phaethon, consistent with the idea that these two bodies have a common origin (Jewitt & Hsieh 2006; Kinoshita et al. 2007).

Recently, Ohtsuka et al. (2008) suggested that another apparently asteroidal object, 1999 YC, may have an orbital association with 2005 UD, 3200 Phaethon, and the Geminid meteoroid stream. In this paper, we present physical observations of 1999 YC. Its colors, size, rotational period, and limits to the ongoing mass loss rate and the fractional active area are compared with those of 2005 UD and 3200 Phaethon.

2. OBSERVATIONS

Observations were taken on the nights of UT 2007 September 4, October 4, 12, 18, and 19 using the University of Hawaii 88 inch (2.2 m) diameter telescope (hereafter, UH 2.2) and the Keck-I 10 m diameter telescope, both located at 4200 m altitude atop Mauna Kea, Hawaii. The UH 2.2 employed a Tektronix 2048 × 2048 pixel charge-coupled device (CCD) camera at the $f/10$ Cassegrain focus. This detector has an image scale of 0.″219 pixel^{-1} and a field of view of approximately 7.′5 × 7.′5. On Keck-I, the Low Resolution Imaging Spectrometer (LRIS) camera (Oke et al. 1995) was used in its imaging mode. This device is equipped with two separate cameras having independent CCD imagers. One is a blue-side CCD having 4096 × 4096 pixels, each 0.″135 pixel^{-1}, and the other is a red-side detector having 2048 × 2048 pixels, each 0.″215 pixel^{-1}. The blue side of LRIS was used to record images in the *B* filter, while images in the *V* and *R* filters were recorded using the red-side detector of LRIS at the same time, which doubled the observational efficiency relative to a single-channel camera.

All images were obtained through the Johnson–Kron–Cousins *BVR*-filter system with the telescopes tracked nonsidereally to follow the motion of 1999 YC at rates about 52″ h^{-1}. Unfortunately, images in the *I* filter could not be obtained at UH 2.2 due to the faintness of 1999 YC and 2005 UD while the *I* filter at the Keck-I 10 m broke shortly before our observing time. Images were corrected by subtracting a bias image and dividing by a bias-subtracted flat-field image. Flat-field images at the UH 2.2 were constructed from scaled, dithered images of the twilight sky. At the Keck-I 10 m we obtained flat fields using artificial light to illuminate the inside of the Keck dome. Photometric calibration was obtained using standard stars from Landolt (1992), including 94-401, 95-98, 92-410, 92-412, L98-627, L98-634, L98-642, L98-646, Mark A1, A2, and A3, and PG2213-006A and C. The median full width at half-maximum (FWHM) measured on 1999 YC varied from ∼0.″6 to 0.″9. An observational log is given in Table 1. Photometry of 2005 UD and 3200 Phaethon was taken in parallel with 1999 YC in order to compare with published observations and to minimize the possibility of systematic differences.

3. OBSERVATIONAL RESULTS

All three objects 1999 YC, 2005 UD, and 3200 Phaethon show point-like images in our data (see Figure 1). Photometry was performed using synthetic circular apertures projected onto the

Table 1
Observation Log

Object	UT Date	Telescope[a]	Integration (s)	Filter	R^b (AU)	Δ^c (AU)	α^d (deg)
1999 YC	2007 Oct 4	UH 2.2	400	1 B, 1 V, 13 R	2.6030	1.9121	18.67
	2007 Oct 12	Keck 10	200	2 × (B & R), 2 × (B & V)	2.6013	1.8185	16.37
	2007 Oct 18	UH 2.2	300	48 R	2.5985	1.7592	14.43
	2007 Oct 19	UH 2.2	300	13 R	2.5979	1.7499	14.08
155140 (2005 UD)	2007 Oct 4	UH 2.2	300	2 B, 2 V, 2 R	2.3767	1.6423	19.81
(3200) Phaethon	2007 Sep 4	UH 2.2	200	1 B, 1 R, 1 I	1.9916	2.0799	28.58
			100	2 B, 3 V, 2 R, 2 I			

Notes.
[a] UH 2.2 = University of Hawaii 2.2 m (88 inch) telescope, Keck 10 = 10 m Keck-I telescope.
[b] Heliocentric distance.
[c] Geocentric distance.
[d] Phase angle.

Table 2
Color Photometry for 1999 YC

Object	Telescope[a]	Date (UT 2007)	Midtime	$B-R$	$B-V$	$V-R$	R
1999 YC	UH 2.2	Oct 4	11.09992	1.07 ± 0.07	...	...	21.15[b]
			11.34678	...	...	0.40 ± 0.06	21.13[b]
	Keck-10	Oct 12	205.20989	1.110 ± 0.013	...	...	21.120 ± 0.008
			205.40086	...	0.734 ± 0.011	...	21.00[b]
			205.47228	...	0.728 ± 0.011	...	20.96[b]
			205.55449	1.112 ± 0.011	...	...	20.911 ± 0.008

Notes.
[a] UH 2.2 = University of Hawaii 2.2 m telescope, Keck 10 = 10 m Keck-I telescope.
[b] R-band magnitude interpolated from the light curve in Figure 4 on UH 2.2 and from the linear fitting on Keck 10.

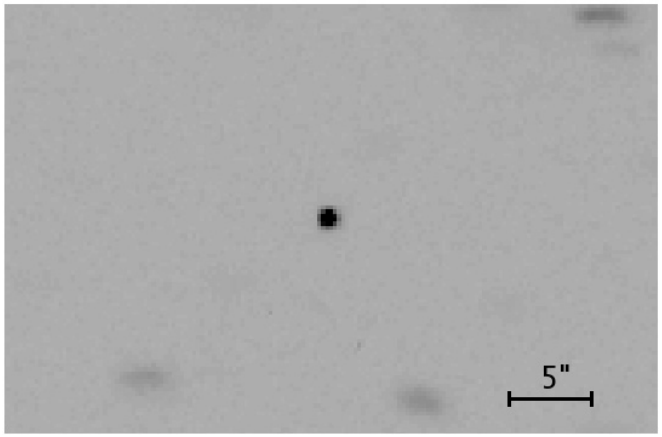

Figure 1. The median-combined R-band image of the asteroid 1999 YC taken by Keck-I 10 m on UT 2007 October 12. The image having a total integration time of 400 s shows no coma. The object with a FWHM of ∼0.″65 is centered within a frame 40″ wide.

sky. Photometry was determined using apertures of radius ∼1.″5 (typically twice the image FWHM), while the sky background was determined within a concentric annulus having projected inner and outer radii of 3.″3 and 6.″6, respectively. Photometric results for 1999 YC are listed in Tables 2 and 3. Colors of 1999 YC are given in Table 4 together with those of 2005 UD, 3200 Phaethon, and solar color indices.

Figure 2 shows the relation between $B-V$ and $V-R$ for various Tholen taxonomy classes measured from 56 near-Earth asteroids (Dandy et al. 2003). The colors of 1999 YC are consistent with C-type asteroids within the uncertainties, and 2005 UD in this work is also similar to the flattened reflectance spectra as seen in C-type asteroids. The colors of 3200 Phaethon measured here agree with numerous independent studies that spectrally classified it as a B- (or F-)type asteroid (Tholen 1985; Luu & Jewitt 1990; Skiff et al. 1996; Lazzarin et al. 1996; Hicks 1998; Dundon 2005; Licandro et al. 2007).

Most published optical colors of 3200 Phaethon and 2005 UD are slightly bluer than the Sun. Bluer colors are uncommon amongst near-Earth asteroids, occurring in about 1 of 23 objects (Jewitt & Hsieh 2006). Kinoshita et al. (2007) found that the color of 2005 UD varies slightly with rotational phase, being bluer than the Sun for 75% of the light curve but neutral (C-type) for the remainder. They speculated that the surface of 2005 UD is heterogeneous perhaps as a result of the splitting phenomenon or of a collision, consistent with being a PGC fragment. Heterogeneity on the surface of 3200 Phaethon was also suggested (Licandro et al. 2007). It shows possible spectral variability due to inhomogeneous compositions caused by the thermal alteration at its small perihelion distance $q \sim 0.14$ AU or by the hydration process (Licandro et al. 2007). Therefore, while 1999 YC appears slightly redder than the rotationally averaged colors of 2005 UD and 3200 Phaethon (Figure 2), the differences are not much larger than either the measurement uncertainties or the reported color variations on 2005 UD. We conclude that the color data are not inconsistent with an association between 1999 YC and the other objects in the dynamically defined PGC (see Table 4).

3.1. Size

Table 3 shows the results of R-band photometry of 1999 YC on the nights of UT 2007 October 4, 18, and 19. The apparent red magnitude m_R was corrected to the absolute red magnitude

Table 3
Light-Curve Photometry through the *R*-Band Filter on UH 2.2

N	Date (UT 2007)	Midtime[a]	Apparent: m_R[b]	Relative[c]
1	Oct 4	10.60783	21.527 ± 0.052	0.002 ± 0.052
2	Oct 4	10.73076	21.393 ± 0.048	−0.160 ± 0.048
3	Oct 4	10.85411	21.260 ± 0.040	−0.269 ± 0.040
4	Oct 4	10.97708	21.198 ± 0.035	−0.315 ± 0.035
5	Oct 4	11.48112	21.102 ± 0.037	−0.395 ± 0.037
6	Oct 4	11.60382	21.282 ± 0.045	−0.220 ± 0.045
7	Oct 4	11.72611	21.270 ± 0.038	−0.232 ± 0.038
8	Oct 4	11.84932	21.378 ± 0.042	−0.131 ± 0.042
9	Oct 4	11.97159	21.537 ± 0.053	0.030 ± 0.053
10	Oct 4	12.09383	21.771 ± 0.080	0.226 ± 0.080
11	Oct 4	12.21696	22.012 ± 0.112	0.350 ± 0.112
12	Oct 4	12.33933	21.788 ± 0.075	0.254 ± 0.075
13	Oct 4	12.46161	21.844 ± 0.070	0.301 ± 0.070
14	Oct 18	346.33945	20.791 ± 0.033	−0.281 ± 0.033
15	Oct 18	346.43490	20.699 ± 0.024	−0.320 ± 0.024
16	Oct 18	346.53053	20.853 ± 0.026	−0.211 ± 0.026
17	Oct 18	346.62621	20.937 ± 0.023	−0.190 ± 0.023
18	Oct 18	346.72193	20.854 ± 0.024	−0.164 ± 0.024
19	Oct 18	346.81773	20.877 ± 0.029	−0.122 ± 0.029
20	Oct 18	346.91605	21.016 ± 0.028	0.005 ± 0.028
21	Oct 18	347.01132	21.124 ± 0.029	0.077 ± 0.029
22	Oct 18	347.10691	21.302 ± 0.039	0.209 ± 0.039
23	Oct 18	347.20252	21.305 ± 0.042	0.302 ± 0.042
24	Oct 18	347.29782	21.330 ± 0.042	0.293 ± 0.042
25	Oct 18	347.39352	21.356 ± 0.044	0.311 ± 0.044
26	Oct 18	347.48865	21.326 ± 0.037	0.282 ± 0.037
27	Oct 18	347.58421	21.216 ± 0.033	0.209 ± 0.033
28	Oct 18	347.67977	21.097 ± 0.032	0.071 ± 0.032
29	Oct 18	347.77528	21.048 ± 0.027	0.035 ± 0.027
30	Oct 18	347.87110	20.951 ± 0.026	−0.041 ± 0.026
31	Oct 18	347.96628	20.636 ± 0.024	−0.361 ± 0.024
32	Oct 18	348.06137	20.858 ± 0.032	−0.139 ± 0.032
33	Oct 18	348.15678	20.764 ± 0.032	−0.237 ± 0.032
34	Oct 18	348.25232	20.786 ± 0.030	−0.200 ± 0.030
35	Oct 18	348.34741	20.731 ± 0.027	−0.233 ± 0.027
36	Oct 18	348.44813	20.662 ± 0.036	−0.322 ± 0.036
37	Oct 18	348.54359	20.788 ± 0.044	−0.195 ± 0.044
38	Oct 18	349.02222	20.737 ± 0.070	−0.255 ± 0.070
39	Oct 18	349.11891	20.852 ± 0.055	−0.138 ± 0.055
40	Oct 18	349.21456	20.852 ± 0.082	−0.139 ± 0.082
41	Oct 18	349.32338	21.210 ± 0.044	0.224 ± 0.044
42	Oct 18	349.41889	21.264 ± 0.048	0.281 ± 0.048
43	Oct 18	349.51430	21.282 ± 0.063	0.298 ± 0.063
44	Oct 18	349.60946	21.356 ± 0.077	0.373 ± 0.077
45	Oct 18	349.70458	21.340 ± 0.052	0.358 ± 0.052
46	Oct 18	349.79988	21.329 ± 0.054	0.348 ± 0.054
47	Oct 18	349.89582	21.186 ± 0.085	0.207 ± 0.085
48	Oct 18	349.99088	21.031 ± 0.047	0.050 ± 0.047
49	Oct 18	350.10853	20.992 ± 0.029	0.033 ± 0.029
50	Oct 18	350.20475	20.891 ± 0.027	−0.072 ± 0.027
51	Oct 18	350.30036	20.742 ± 0.023	−0.241 ± 0.023
52	Oct 18	350.39558	20.784 ± 0.024	−0.198 ± 0.024
53	Oct 18	350.49086	20.754 ± 0.022	−0.229 ± 0.022
54	Oct 18	350.58617	20.731 ± 0.022	−0.249 ± 0.022
55	Oct 18	350.68131	20.725 ± 0.020	−0.256 ± 0.020
56	Oct 18	350.77684	20.734 ± 0.021	−0.250 ± 0.021
57	Oct 18	350.87236	20.699 ± 0.022	−0.282 ± 0.022
58	Oct 18	350.96777	20.722 ± 0.021	−0.259 ± 0.021
59	Oct 18	351.06372	20.773 ± 0.025	−0.204 ± 0.025
60	Oct 18	351.16056	20.772 ± 0.024	−0.210 ± 0.024
61	Oct 18	351.25728	20.892 ± 0.029	−0.088 ± 0.029
62	Oct 19	370.92062	20.691 ± 0.026	−0.296 ± 0.026
63	Oct 19	371.01599	20.731 ± 0.025	−0.264 ± 0.025
64	Oct 19	371.11155	20.845 ± 0.026	−0.225 ± 0.026
65	Oct 19	371.20698	20.842 ± 0.026	−0.222 ± 0.026
66	Oct 19	371.30237	20.794 ± 0.025	−0.242 ± 0.025

Table 3
(Continued)

N	Date (UT 2007)	Midtime[a]	Apparent: m_R[b]	Relative[c]
67	Oct 19	371.39801	20.852 ± 0.029	−0.219 ± 0.029
68	Oct 19	371.49356	20.863 ± 0.022	−0.119 ± 0.022
69	Oct 19	371.58887	20.880 ± 0.031	−0.139 ± 0.031
70	Oct 19	371.68409	20.897 ± 0.028	−0.071 ± 0.028
71	Oct 19	371.77922	20.994 ± 0.034	−0.005 ± 0.034
72	Oct 19	371.87735	20.967 ± 0.038	0.019 ± 0.038
73	Oct 19	371.97288	21.184 ± 0.037	0.235 ± 0.037
74	Oct 19	372.07014	21.273 ± 0.040	0.322 ± 0.040

Notes.
[a] Time since UT 2007 October 4. The middle of integration times is taken.
[b] Apparent magnitude measured in the *R*-band image.
[c] Relative red magnitude to seven field stars in background.

Table 4
Color Results of the PGC

Object	$B-V$	$V-R$	$R-I$	Source
1999 YC	0.71 ± 0.04	0.36 ± 0.03	...	(1)
2005 UD	0.68 ± 0.01	0.39 ± 0.02	...	(1)
	0.66 ± 0.03	0.35 ± 0.02	0.33 ± 0.02	(2)
	0.63 ± 0.01	0.34 ± 0.01	0.30 ± 0.01	(3)
Phaethon	0.61 ± 0.01	0.34 ± 0.03	0.27 ± 0.04	(1)
	0.59 ± 0.01	0.35 ± 0.01	0.32 ± 0.01	(4)
	...	0.34	...	(5)
Solar colors	0.67	0.36	0.35	(2)

References. (1) This work, (2) Jewitt & Hsieh (2006), (3) Kinoshita et al. (2007), (4) Dundon (2005), (5) Skiff et al. (1996).

$m_R(1, 1, 0)$ using

$$m_R(1, 1, 0) = m_R - 5\log(r\,\Delta) - \beta\alpha, \quad (1)$$

where r and Δ are the heliocentric and geocentric distances in AU, α is the phase angle in degrees (Sun–target–observer), and β is the phase coefficient.

We did not sample the full rotational light-curve variation on each epoch of observation. Therefore, we cannot simply use the mean or median brightness at each epoch in order to measure the phase variation. Instead, we determined the linear phase coefficient, β, in mag deg^{-1}, from the better-observed brightness maxima in night-to-night light curves from m_R in Table 3 (N = 4, 5 on October 4; N= 14–16, 30–32, 56–58 on October 18; 62–64 on October 19, where N shows the file number in Table 3).

Figure 3 shows the correlation between the phase angle and the reduced apparent red magnitudes corrected to R = Δ = 1 AU by Equation (1). The derived coefficient, β = 0.044 ± 0.002 mag deg^{-1}, is consistent with a low albedo, as observed in cometary nuclei (Lamy et al. 2004), and similar to the C-type asteroids (β = 0.041 ± 0.003) at phase angles of 5° < α < 25° (Belskaya & Shevchenko 2000).

We used the absolute magnitudes, $m_R(1, 1, 0)$, to calculate the equivalent circular diameter, D_e, using (Russell 1916)

$$D_e(\mathrm{km}) = \left[\frac{1140}{p_v^{1/2}}\right] 10^{(-0.2 m_R(1,1,0))}, \quad (2)$$

in which we have taken the apparent red magnitude of the Sun as m_R = −27.1 (Cox 2000). We adopt the albedo p_v ($\approx p_R$) = 0.11 ± 0.02 as obtained from infrared observations of 3200 Phaethon (Green et al. 1985).

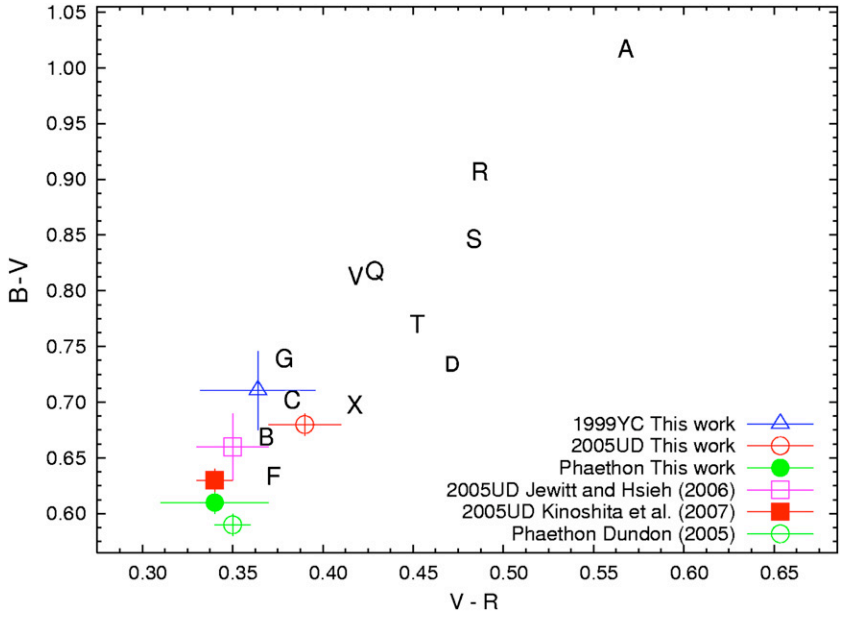

Figure 2. Color plots of $V - R$ vs. $B - V$ for PGC and near-Earth asteroids within various Tholen taxonomic classes (Dandy et al. 2003).

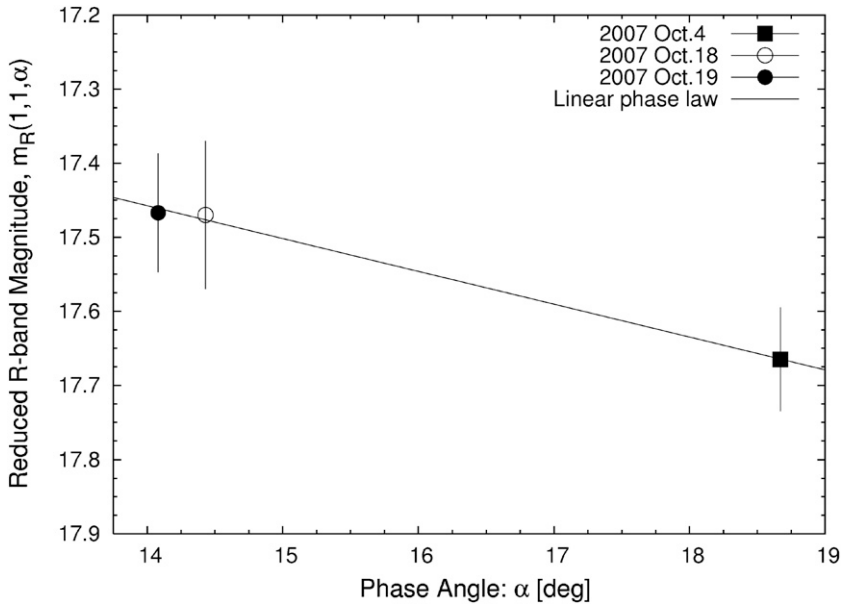

Figure 3. The linear-phase function for 1999 YC. The solid curve shows a phase coefficient $\beta = 0.044 \pm 0.002$ mag deg^{-1} determined by fitting data from UT 2007 October 4, 18, and 19.

Table 5 lists the absolute magnitudes $m_R(1, 1, 0)$ and the resulting equivalent circular diameters D_e of 1999 YC, 2005 UD, and 3200 Phaethon. The table shows that 1999 YC and 2005 UD are similar in size and each is about one-quarter of the diameter (and, presumably, 4^{-3} ~2% of the mass) of 3200 Phaethon.

Table 5
Absolute Red Magnitude $m_R(1, 1, 0)$ and Equivalent Circular D_e

Object	$m_R(1, 1, 0)$	D_e (km)	Source
1999 YC	16.96 ± 0.03	1.4 ± 0.1	(1)
2005 UD	17.23 ± 0.03	1.2 ± 0.1	(1)
	17.13 ± 0.03	1.3 ± 0.1	(2)
Phaethon	14.22 ± 0.01	4.9 ± 0.4	(1)
	$\sim 14.3 \pm 0.1$	4.7 ± 0.5	(3), (4)

References. (1) This work, (2) Jewitt & Hsieh (2006), (3) Green et al. (1985), (4) Dundon (2005).

3.2. Light Curve

In order to find the rotation period for 1999 YC, the phase dispersion minimization (PDM) technique (Stellingwerf 1978) was used both on the absolute red magnitudes, $m_R(1, 1, 0)$, and on the relative red magnitudes defined as excursions from the median magnitude measured each night. The PDM in the NOAO IRAF software package provided us with several possible light-curve periods and enabled us to visually examine the data for each period. The most likely rotational period was determined by the smallest value of theta (see details in Stellingwerf 1978), namely a single-peaked light curve of period $P_0 = 2.247$ h. Other possible rotational periods are related to multiples of

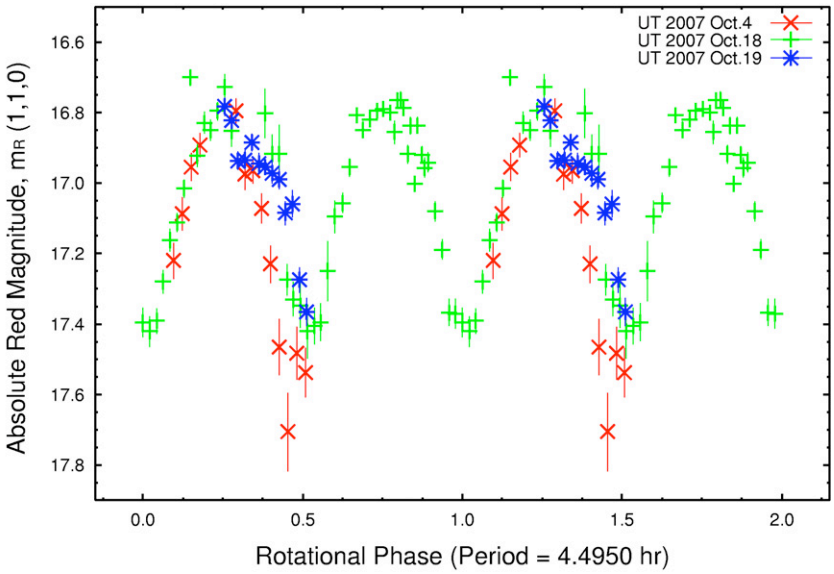

Figure 4. Rotational phase vs. absolute red magnitude variation of 1999 YC observed on UT 2007 October 4, 18, and 19. $m_R(1, 1, 0)$ is phased to the double-peaked rotational period of $P_{rot} = 4.4950 \pm 0.0010$ h.

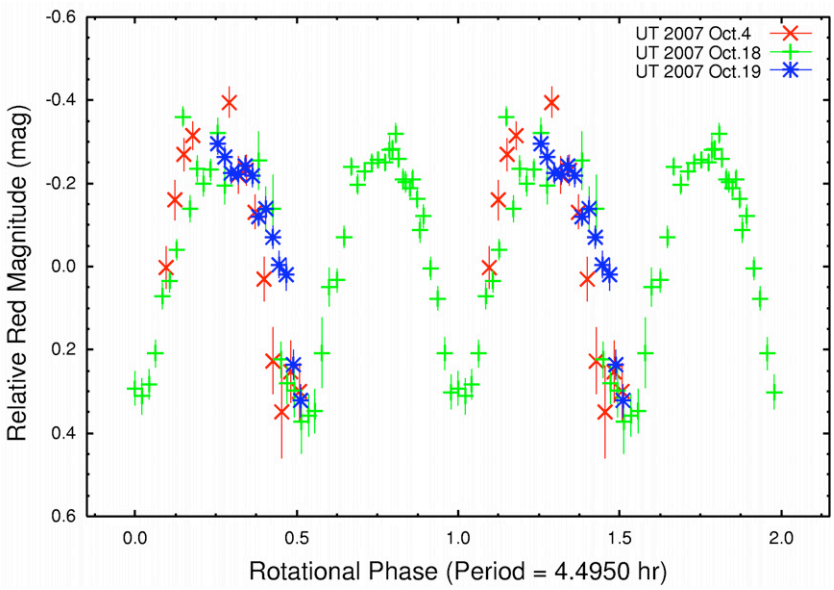

Figure 5. Rotational phase vs. relative red magnitude variation of 1999 YC observed on UT 2007 October 4, 18, and 19, phased to the double-peaked rotational period of $P_{rot} = 4.4950 \pm 0.0010$ h. Magnitudes from the different nights are phased and plotted relative the median magnitude of each night.

P_0. The light curves of most small bodies in the solar system are double-peaked, resulting from elongated shapes rather than from strong albedo markings. We assume that the light curve of 1999 YC is double-peaked and so conclude that the true rotation period is $P_{rot} = 2P_0 = 4.4950$ h (Figures 4, 5). The uncertainty on the period is estimated as 0.0010 h, by examination of the acceptable phased light curves. This is comparable to the 5.249 h period of 2005 UD and the 3.59 h period of 3200 Phaethon (see Table 6). Pravec et al. (2002) computed the mean spin rate versus diameter to find $P_{rot} \sim 5.0 \pm 0.6$ h for asteroids of diameter $D_e \sim 1$ km. We conclude that, although short, the rotation period of 1999 YC is not unusual for asteroids of a comparable size.

The maximum photometric range of 1999 YC is $\Delta m_R = 0.69 \pm 0.05$, giving a minimum axis ratio of the body. Assuming that the amplitude is shown by the largest and smallest faces presented during the rotation of an elongated body, the ratio of the long-to-short axis of 1999 YC projected on the plane of the sky is expressed by

$$10^{0.4\Delta m_R} = \frac{a}{b} = 1.89 \pm 0.09, \quad (3)$$

where a is the long axis and b is the short axis. While 1999 YC is more elongated than either 2005 UD ($a/b = 1.45 \pm 0.06$) or 3200 Phaethon ($a/b \sim 1.45$; Jewitt & Hsieh 2006; Dundon 2005), the observed differences cannot be accurately interpreted because of the unknown spin vectors of these bodies and the effects of projection.

A critical density ρ_c can be derived from $\rho_c = 1000$ (3.3 h/P_{rot})^2 for a spherical body with a given rotation period in hour P_{rot}, by equating the acceleration of gravity at the surface with the centripetal acceleration at the equator. For an elongated body like 1999 YC, the acceleration of gravity at the tip of the long axis a is reduced by a factor about equal to the axis

Table 6
Physical properties of 1999 YC, 2005 UD, and 3200 Phaethon

Quantity	Symbol	1999 YC[a]	2005 UD[b]	3200 Phaethon[c,d]
Semimajor axis	a	1.422	1.275	1.271
Perihelion	q	0.241	0.163	0.140
Eccentricity	e	0.831	0.872	0.890
Inclination	i	38.16	28.75	22.16
Rotational period (h)	$P_{\rm rot}$	4.495	5.249	3.59
Photometric range (mag)	$m_{\rm R}$	0.69 ± 0.05	0.40 ± 0.05	0.4
Critical density (kg m^{-3})	ρ_c	1000	570	1200
Mass loss rate (kg s^{-1})	$\dot{M}$	0.001	0.01	0.01
Fractional active area	f	$<10^{-3}$	$<10^{-4}$	$<10^{-5}$

Notes. Orbital data are from Ohtsuka et al. (2006) and NASA JPL HORIZON.
[a] This work.
[b] Jewitt & Hsieh (2006).
[c] Dundon (2005).
[d] Hsieh & Jewitt (2005).

ratio, b/a, compared to that of a sphere of the same density and radius (Harris 1996; Pravec & Harris 2000). Therefore, a critical density for an elongated body is described as

$$\rho_c \approx 1000 \left(\frac{3.3\,\mathrm{h}}{P_{\rm rot}}\right)^2 \left(\frac{a}{b}\right), \quad (4)$$

where $P_{\rm rot}$ is in hours. The critical density is a lower limit in the sense that a less dense body with the observed period and axis ratio would be in a state of internal tension against centripetal acceleration. The critical densities are compared in Table 6.

One additional feature of the light curve shown in Figures 4 and 5 is worthy of note. The data from UT 2007 October 4 do not fit those from UT 2007 October 18 and 19 quite so well as the latter two nights considered alone. This could simply be because 1999 YC was nearly a magnitude fainter on the first date of observation, and therefore the effects of photometric uncertainties in the measurements are proportionally larger. Alternatively, it is possible that the slightly discrepant shape of the light curve from UT 2007 October 4 is a result of non-principal axis rotation of 1999 YC. The latter is to be expected if 1999 YC is a recently produced fragment, because splitting of the nucleus should naturally produce excited rotational states and the timescale for the damping of nutation by internal friction is very long for bodies as small as 1999 YC (Burns & Safronov 1973). For example, for a rubble pile structure, the damping time is $T_{\rm d} = 0.24\ P_{\rm rot}^3/r_{\rm obj}^2$ (in millions of years) (Sharma et al. 2005). Substituting $P_{\rm rot}$ and $r_{\rm obj}$ for 1999 YC, we estimate $T_{\rm d} \sim 10^7$ yr. This is longer than the dynamical lifetime of 10^6 yr (Froeschle et al. 1995) and *much* longer than the estimated $\sim 10^3$ yr age of the Geminid stream, implying that precessional motions acquired at formation would not yet have been damped by internal friction. The same considerations apply to 2005 UD and 3200 Phaethon and non-principal axis rotation should be a general feature of these and other PGC fragments. Still, better temporal coverage will be needed to unambiguously detect non-principal axis rotations.

3.3. Surface Brightness Model

To search for a coma in 1999 YC, we compared its measured surface brightness profile with the profiles of unresolved field stars and with a seeing-convolved profile of a model comet. Because of the non-sidereal motion of 1999 YC, the images of background sources appear trailed in the data and so the surface brightness must be treated using the procedures of Luu & Jewitt (1992).

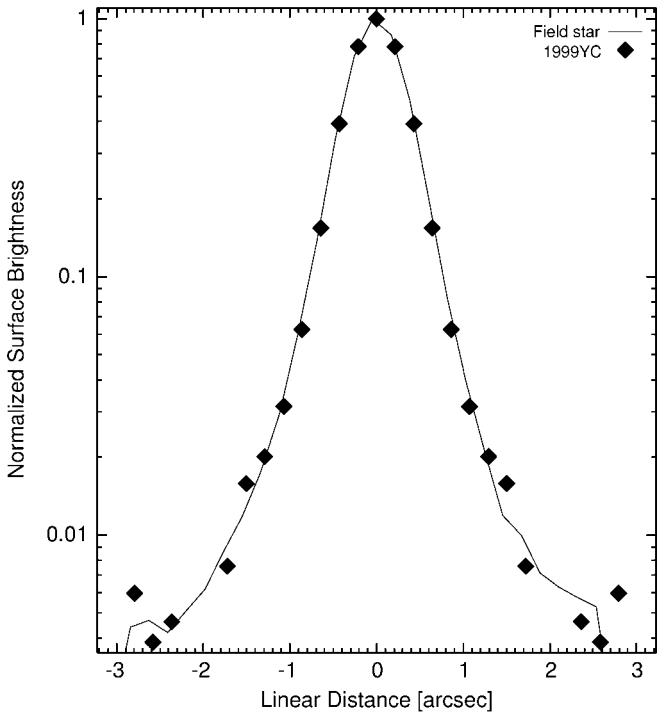

Figure 6. Normalized 1D surface brightness profiles of 1999 YC and a field star.

Firstly, to determine one-dimensional (1D) surface brightness profiles of the asteroid and the field star, we selected two *R*-band images taken using Keck-I on the night of UT 2007 October 12 (combined integration time = 400 s, see Figure 1) because the Keck signal-to-noise ratio (S/N $\geqslant$ 100) is greater than from the UH 2.2 (S/N $\simeq$ 20–30). Each image was rotated using a fifth-order polynomial interpolation so the field star trail was aligned parallel to the pixel rows in the image frame and then median combined into a single image (having FWHM $\sim 0''.65$). Then, 1D surface brightness profiles of 1999 YC and a field star were measured in the direction perpendicular to the trail. Each profile was averaged along the rows over the entire width of the asteroid and the field star after subtracting sky. Both normalized profiles are similar, although with small differences attributed to noise in the data (Figure 6).

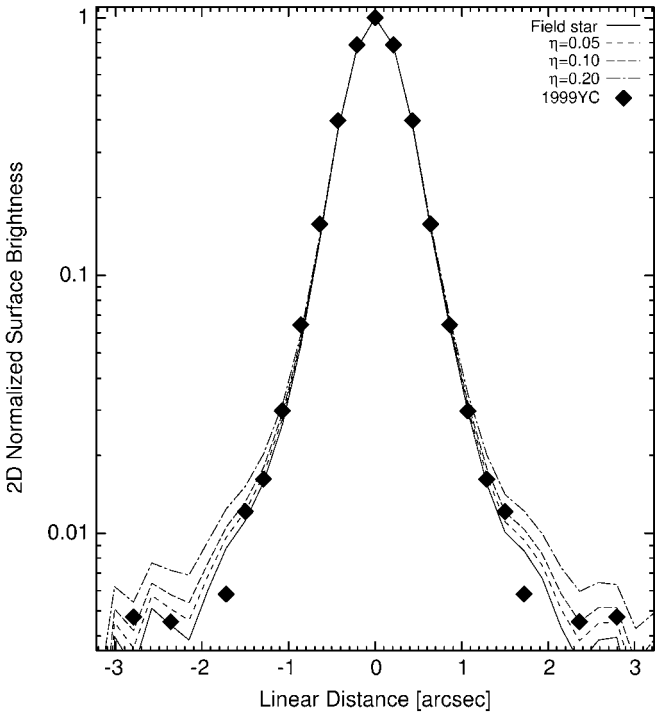

Figure 7. 2D Surface brightness models that compare the 1999 YC's profile with seeing-convolved models having $\eta = 0.05$, 0.10, and 0.20 (see Section 3.3.)

Secondly, to set quantitative limits to coma in 1999 YC, we compared the two-dimensional (2D) point-spread function (PSF) of the asteroid with seeing convolved model profiles of the comet. The seeing was determined from the 2D PSF of a field star, and convolved with simple comet models of "nucleus plus coma." In model images of 100 ×100 pixels, the nucleus was represented by a spike located at the central pixel and the spherically symmetric coma. The parameter η defined as the ratio of the coma cross section C_c to the nucleus cross section C_n, which corresponds to the ratio of the flux density scattered by the coma I_c to the flux density scattered by the nucleus cross section I_n, was able to characterize varying coma-activity levels on preconvolution models (Luu & Jewitt 1992), and expressed as

$$\eta = \frac{C_c}{C_n} = \frac{I_c}{I_n}, \qquad \eta \geqslant 0. \tag{5}$$

The intensity I_c of each pixel in the coma was determined by $I_c = K/r$ as a function of the surface brightness, where K is a constant of proportionality and r is the distance from the nucleus. The parameter η can take $\eta \geqslant 0$, with $\eta = 0$ indicating a bare nucleus (no coma) and $\eta = 1$ indicating coma and nucleus having equal cross sections.

Figure 7 shows convolution models with coma levels of $\eta = 0.05$, 0.10, and 0.20, from which we estimate an upper limit $\eta_{\rm lim} \lesssim 0.1$. Assuming that the mass loss is ongoing and isotropic, the rate can be expressed as a function of the parameter η (Luu & Jewitt 1992):

$$\dot{M} = \frac{dM}{dt} = \frac{1.0 \times 10^{-3} \pi \rho \bar{a} \eta_{\rm lim} r_{\rm obj}^2}{\phi R^{\frac{1}{2}} \Delta}, \tag{6}$$

where $\rho = 1000$ kg m^{-3} is the assumed grain density, $\bar{a} = 0.5 \times 10^{-6}$ m is the assumed grain radius, $r_{\rm obj} = 700$ m is 1999 YC's radius, ϕ is the reference photometry aperture radius of 50 pixels (10.″95) and R and Δ are given in Table 1. The mass loss rate was calculated as $\dot{M} \lesssim 2.4 \times 10^{-3}$ kg s^{-1} with $\eta_{\rm lim} \lesssim 0.1$.

It is not likely that water ice survives on the surface of 1999 YC or any body with a similarly small perihelion distance. Nevertheless, it is interesting to compute the maximum allowable fraction of the surface that could be occupied by water ice while remaining consistent with the point-like surface brightness profile of the object.

To do this, we convert $\dot{M}$ into the fraction of active area on the surface of the object, f, via

$$f = \frac{\dot{M}}{4\pi r_{\rm obj}^2 \mu dm/dt}, \tag{7}$$

where $\mu = 1$ is the assumed dust-to-gas ratio. Under the assumption that volatile material (=water ice) exists, the specific sublimation mass loss rate of water, dm/dt in kg m^{-2} s^{-1}, is calculated from the heat balance equation,

$$\frac{F_\odot (1 - A)}{R^2} = \chi [\epsilon \sigma T^4 + L(T) dm/dt]. \tag{8}$$

Here, $F_\odot = 1365$ W m^{-2} is the solar constant, R (in AU) is the heliocentric distance, $A = 0.11$ is the assumed bond albedo (Green et al. 1985), $\epsilon = 0.9$ is the assumed emissivity, $\sigma = 5.67 \times 10^{-8}$ W m^{-2} K^{-4} is the Stefan–Boltzmann constant, and T in K is the equilibrium temperature. The latent heat of sublimation for water $L(T) = (2.875 \times 10^6) - (1.111 \times 10^3)T$ in J kg^{-1} is taken from the fit to $L(T)$ in Delsemme & Miller (1971). The parameter $1 \leqslant \chi \leqslant 4$ represents the distribution of solar energy over the surface of the object, where $\chi = 1$ corresponds to a flat slab facing the Sun, $\chi = 2$ to the standard thermal model (slow rotator), and $\chi = 4$ to an isothermal sphere. The term on the left represents the flux of energy absorbed from the Sun. The terms on the right represent energy lost from the nucleus surface by radiation and by latent heat of sublimation. In this first-order calculation, thermal conduction is neglected.

The specific sublimation mass loss rate can be derived iteratively using the temperature-dependent water vapor pressure given by Fanale & Salvail (1984). At 2.6 AU, assuming a flat slab model ($\chi = 1.0$), the maximum specific sublimation mass loss rate is $dm/dt = 4.3 \times 10^{-5}$ kg m^{-2} s^{-1} and the temperature is 190 K. On the other hand, minimum values of 9.7×10^{-7} kg m^{-2} s^{-1} and 170 K are found using the isothermal model ($\chi = 4$), giving the maximum fraction of active area $f \sim 4.0 \times 10^{-4}$ using Equation (7).

Figure 8 represents the radius (km) versus fractional active area f for 1999 YC, 2005 UD, 3200 Phaethon with determinations of f for 27 Jupiter family comets (JFCs) (Tancredi et al. 2006). The small active surface fractions of the PGC candidates are obvious, with upper limits of $f < 10^{-3}$ on 1999 YC, on 2005 UD with $f < 10^{-4}$ (Jewitt & Hsieh 2006), and on 3200 Phaethon with $f < 10^{-5}$ (Hsieh & Jewitt 2005). Relatively small active fractions are found in 28P/Neujmin ($f = 0.001$) and in 49P/Arend-Rigaux ($f = 0.007$), although these bodies are an order of magnitude larger than 1999 YC. For bodies of a comparable size, the upper limits to f on PGC are still smaller by more than one order of magnitude than on JFCs.

4. DISCUSSION

The tiny limiting mass loss rates derived from observations of 1999 YC, 2005 UD, and 3200 Phaethon (Table 6) can be compared with the total mass of the Geminid meteoroid

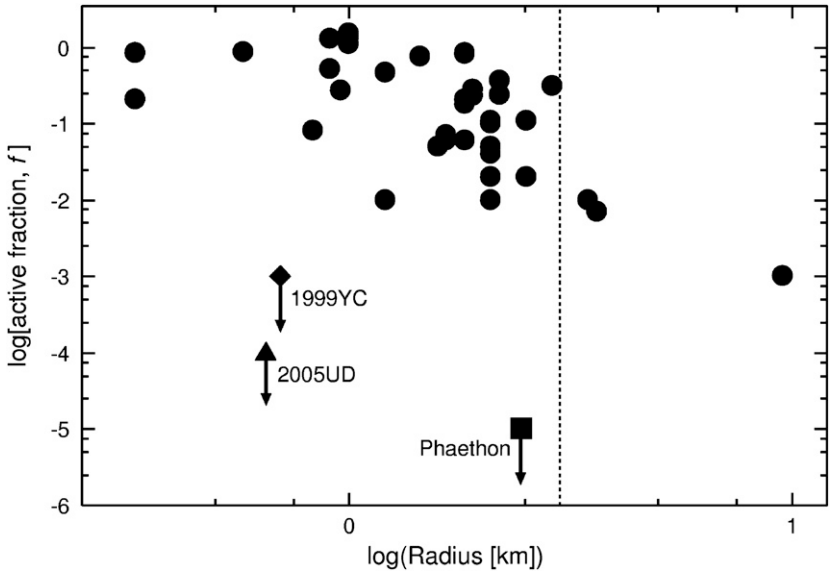

Figure 8. Radius vs. fractional active area, f. For JFCs with $r_{obj} \leqslant 3$ km (vertical dashed line), f is an order of magnitude larger than the maximum active fraction limit found in 1999 YC (see Section 3.3).

stream. The stream has an age estimated dynamically to be a few thousand years at most (Jones 1978; Fox et al. 1982; Jones & Hawkes 1986; Gustafson 1989; Williams & Wu 1993; Ryabova 2001; see also the summary in Jenniskens 2006) and the total mass is $\sim 10^{12}$–10^{13} kg (Hughes & McBride 1989; Jenniskens 1994). The steady mass loss at the maximum rates allowed by the optical data, namely 10^{-2} kg s^{-1} (see Table 6), would deliver only $\sim 3 \times 10^{8}$ kg in 1000 yr. Therefore, the large mass of the Geminid meteoroid stream and the small allowable values of the current mass production rates together point to the origin of the stream by the catastrophic breakup of the parent body, not by steady disintegration at the observed rate (Jewitt & Hsieh 2006) (also see Jenniskens 2008).

However, the mechanism responsible for the breakup of the PGC parent body remains unknown. Jewitt & Hsieh (2006) speculated that ice sublimation in the core of the PGC parent body could be responsible for its disintegration if the sublimation gas pressure substantially exceeded the hydrostatic pressure (also see Samarasinha 2001). This is possible because (a) the timescale for heat to conduct from the surface to the core is smaller than the expected dynamical lifetime provided the radius is $r \leqslant 7$ km and (b) the orbitally-averaged temperature of a body in a PGC-like orbit is high enough to promote strong sublimation of water ice even in the core. The mainbelt comets orbit in the asteroid belt (they have asteroid-like $T_J > 3$) and contain ice (Hsieh & Jewitt 2006). If such an object were deflected into a planet-crossing orbit with a small perihelion distance, like the PGC bodies, it is conceivable that a period of strong surface outgassing might be followed, after a thermal diffusion time, by disruption due to sublimation of ice in the core. Another possibility is that spin-up caused by torques from non-central mass loss in such an object might result in centripetal disruption and breakup, although whether this would produce a Geminid-like stream as opposed to a few large chunks is far from clear. Still another possibility is that spin-up and disruption occur through the Yarkovsky–O'Keefe–Radzievskii–Paddack (YORP) effect: the timescale for the action of YORP is short for bodies, like 1999 YC and the other members of the PGC, having a small perihelion distance and large eccentricities (Scheeres 2007).

Measurements of the Na content of the Geminid meteoroids provide an indicator of the effects of solar heating. This is because Na is a relatively volatile (temperature-sensitive) and abundant (easy to detect) element. Spectroscopic observations of Geminid meteors show an extreme diversity of Na contents, from strong depletion of Na abundance in some (~7% of the solar abundance) (Kasuga et al. 2005) to Sun-like values in others (Harvey 1973). Line intensity ratios in the Geminids also show a wide range of Na content, from undetectable to strong (Borovička et al. 2005). Kasuga et al. (2006a) investigated the thermal desorption of Na in meteoroids in meteor streams during their orbital motion in interplanetary space. They found it unlikely that the Na content has been modified thermally because the peak temperatures of the meteoroids, even when at $q \sim 0.14$ AU, are lower than the sublimation temperature of alkali silicates (~900 K) (Kasuga et al. 2006a). Therefore, the diversity of Na abundances observed in Geminid meteoroids must have another origin, perhaps related to the thermal evolution of 3200 Phaethon or the larger sized fragments themselves. For example, the Na content may relate to the position in the parent body before the meteoroids were ejected. The physical properties of meteoroids from the surface regions could be changed by compaction associated with loss of volatiles (Beech 1984). These Geminid meteoroids would be stronger and have higher bulk density (Verniani 1967; Wetherill 1986; Babadzhanov 2002). On the other hand, Geminids from the interior might be relatively fresh uncompacted and volatile rich, with the Na preserving more Sun-like values. Eventually, the true natures of PGC fragments and ice-rich asteroids (dormant comets) may be revealed by missions resembling NASA's "Deep Impact" (A'Hearn et al. 2005; Kasuga et al. 2006b).

5. SUMMARY

Optical observations of asteroid 1999 YC, a suggested member of the PGC, give the following results.

1. Optical colors measured for 1999 YC are nearly neutral, consistent with those of the taxonomic C-type asteroids and slightly redder than the neutral-blue colors found on other PGC bodies.

2. The absolute red magnitude is $m_R(1, 1, 0) = 16.96 \pm 0.03$, giving the equivalent circular diameter $D_e = 1.4 \pm 0.1$ km assuming the same geometric albedo as 3200 Phaethon ($p_R = 0.11$).
3. The light curve of 1999 YC has the double-peaked period of $P_{rot} = 4.4950 \pm 0.0010$ h. The photometric range of $\Delta m_R = 0.69 \pm 0.05$ mag corresponds to an axis ratio of 1.89 ± 0.09, suggesting an elongated body with the critical density $\geqslant 1000$ kg m^{-3}.
4. No evidence of lasting mass loss was found from the surface brightness profiles in imaging data. The maximum mass loss rate is $\sim 10^{-3}$ kg s^{-1} which corresponds to the fractional active area $f < 10^{-3}$.
5. Catastrophic breakup or comet-like disintegration of a precursor body is suggested because the mass loss rates are too small to form the massive Geminid meteoroid stream in the steady state given the 1000 yr dynamical lifetime.

T.K. is grateful to Robert Jedicke for his enthusiastic encouragement in studies at the Institute for Astronomy, UH. We thank our colleagues Bin Yang, Pedro Lacerda (UH), Katsuhito Ohtsuka (Tokyo Meteor Network), Masanao Abe, Sunao Hasegawa, Kyoko Kawakami, and Taichi Kawamura (ISAS/JAXA) for useful discussions. We appreciate financial support to T.K. from the JSPS Research Fellowships for young scientists and to D.J. from NASA's Planetary Astronomy Program. Lastly, we thank Peter Jenniskens for his prompt review.

REFERENCES

A'Hearn, M. F., et al. 2005, Science, 310, 258
Babadzhanov, P. B. 1994, in ASP Conf. Ser. 63, ed. Y. Kozai, R. P. Binzel, & T. Hirayama (San Francisco, CA: ASP), 168
Babadzhanov, P. B. 2002, A&A, 384, 317
Beech, M. 1984, MNRAS, 211, 617
Belskaya, I. N., & Shevchenko, V. G. 2000, Icarus, 147, 94
Boehnhardt, H. 2004, in Comets II, 745, ed. M. C. Festou, H. U. Keller, & H. A. Weaver (Tucson, AZ: Univ. Arizona Press), 301
Borovička, J., Koten, P., Spurný, P., Boček, J., & Štork, R. 2005, Icarus, 174, 15
Burns, J. A., & Safronov, V. S. 1973, MNRAS, 165, 403
Chen, J., & Jewitt, D. 1994, Icarus, 108, 265
Cox, A. N. 2000, Allen's Astrophysical Quantities, (New York: Springer)
Dandy, C. L., Fitzsimmons, A., & Collander Brown, S. J. 2003, Icarus, 163, 363
Delsemme, A. H., & Miller, D. C. 1971, Planet. Space Sci., 19, 1229
Dundon, L. 2005, M.S. Thesis Univ. of Hawaii
Fanale, F. P., & Salvail, J. R. 1984, Icarus, 60, 476
Fox, K., Williams, I. P., & Hughes, D. W. 1982, MNRAS, 199, 313
Froeschle, C., Hahn, G., Gonczi, R., Morbidelli, A., & Farinella, P. 1995, Icarus, 117, 45
Green, S. F., Meadows, A. J., & Davies, J. K. 1985, MNRAS, 214, 29P
Gustafson, B. A. S. 1989, A&A, 225, 533
Harris, A. W. 1996, Lunar Planet Sci., 27, 493
Harvey, G. A. 1973, NASA SP, 319, 103
Hicks, M. D., Fink, U., & Grundy, W. M. 1998, Icarus, 133, 69
Hsieh, H. H., & Jewitt, D. 2006, Science, 312, 561
Hsieh, H. H., & Jewitt, D. 2005, ApJ, 624, 1093
Hughes, D. W., & McBride, N. 1989, MNRAS, 240, 73
Jenniskens, P. 2006, Meteor Showers and their Parent Comets (Cambridge: Cambridge Univ. Press)
Jenniskens, P. 1994, A&A, 287, 990
Jenniskens, P. 2008, Earth Moon Planets, 102, 505
Jewitt, D. 2004, in Comets II, 745, ed. M. C. Festou, H. U. Keller, & H. A. Weaver (Tucson, AZ: Univ. Arizona Press), 659
Jewitt, D., & Hsieh, H. H. 2006, AJ, 132, 1624
Jones, J. 1978, MNRAS, 183, 539
Jones, J., & Hawkes, R. L. 1986, MNRAS, 223, 479
Kasuga, T., Watanabe, J., & Ebizuka, N. 2005, A&A, 438, L17
Kasuga, T., Yamamoto, T., Kimura, H., & Watanabe, J. 2006a, A&A, 453, L17
Kasuga, T., Watanabe, J., & Sato, M. 2006b, MNRAS, 373, 1107
Kinoshita, D., et al. 2007, A&A, 466, 1153
Lamy, P. L., Toth, I., Fernandez, Y. R., & Weaver, H. A. 2004, in Comets II, 745, ed. M. C. Festou, H. U. Keller, & H. A. Weaver (Tucson, AZ: Univ. Arizona Press), 223
Licandro, J., Campins, H., Mothé-Diniz, T., Pinilla Alonso, N., & de León, J. 2007, A&A, 461, 751
Landolt, A. U. 1992, AJ, 104, 340
Lazzarin, M., Barucci, M. A., & Doressoundiram, A. 1996, Icarus, 122, 122
Luu, J. X., & Jewitt, D. C. 1990, AJ, 99, 1985
Luu, J. X., & Jewitt, D. C. 1992, Icarus, 97, 276
Ohtsuka, K., Ito, T., Arakida, H., & Yoshikawa, M. 2008, M&PSA, 43, 5055
Ohtsuka, K., Sekiguchi, T., Kinoshita, D., Watanabe, J. I., Ito, T., Arakida, H., & Kasuga, T. 2006, A&A, 450, L25
Oke, J. B., et al. 1995, PASP, 107, 375
Pravec, P., & Harris, A. W. 2000, Icarus, 148, 12
Pravec, P., Harris, A. W., & Michalowski, T. 2002, in Asteroids III, ed. W. F. Bottke, Jr., et al. (Tucson, AZ: Univ. Arizona Press), 113
Ryabova, G. O. 2001, ESA SP-495, 77
Russell, H. N. 1916, ApJ, 43, 173
Samarasinha, N. H. 2001, Icarus, 154, 540
Scheeres, D. J. 2007, Icarus, 188, 430
Sharma, I., Burns, J. A., & Hui, C.-Y. 2005, MNRAS, 359, 79
Skiff, B. A., Buie, M. W., & Bowell, E. 1996, BAAS, 28, 1104
Stellingwerf, R. F. 1978, ApJ, 224, 953
Tancredi, G., Fernández, J. A., Rickman, H., & Licandro, J. 2006, Icarus, 182, 527
Tholen, D. J. 1985, IAU Circ., 4034, 2
Verniani, F. 1967, Smith Contr. Astrophys., 10, 181
Wetherill, G. W. 1986, Meteoritics, 21, 537
Whipple, F. L. 1983, IAU Circ., 3881, 1
Wiegert, P. A., Houde, M., & Peng, R. 2008, Icarus, 194, 843
Williams, I. P., & Wu, Z. 1993, MNRAS, 262, 231